COMMISSARIAT A L'ENERGIE ATOMIQUE

CENTRE D'ETUDES NUCLEAIRES DE SACLAY
Service de Documentation
F91191 GIF SUR YVETTE CEDEX

CEA-CONF - -9766

M1

STUDY OF NON STOICHIOMETRIC PURE AND Zr-DOPED YTTRIA SURFACES BY X-RAY PHOTOELECTRON SPECTROSCOPY AND SCANNING ELECTRON MICROSCOPY

GAUTIER M.- DURAUD J.P.- JOLLET F.- THROMAT N.- MAIRE P.- LE GRESSUS C.

CEA Centre d'Etudes Nucleaires de Saclay, 91 - Gif-sur-Yvette (FR). Dept. de Physico-Chimie

Communication présentée à : Surface and Interface of Ceramics Materials Summer School
Oleron (FR)
4-16 Sep 1988

STUDY OF NON STOICHIOMETRIC PURE AND Zr-DOPED YTTRIA SURFACES BY X-RAY PHOTOELECTRON SPECTROSCOPY AND SCANNING ELECTRON MICROSCOPY

M. Gautier, J.P. Duraud, F. Jollet, N. Thromat,
Ph. Maire, C. Le Gressus
IRDI/DESICP/DPC/SPCM
Centre d'Etudes Nucléaires de Saclay
91191 Gif-sur-Yvette Cedex, France

ABSTRACT. Surfaces of oxygen-deficient yttrium oxide, pure or Zr-doped, have been studied by means of X-ray photoelectron spectroscopy and scanning electron microscopy.

The bulk local geometric structure of these non-stoichiometric compounds was previously determined around the Y atom by an EXAFS (Extended X-ray absorption fine structure) study.

The local electronic structure around both Y and O, at the surface, was investigated by X-ray photoelectron spectroscopy.

The partial transfer of the electronic distribution between the anion and the cation was probed using the Auger parameter.

Coupling of these experiments with microscopic observations show that :

- In the pure oxygen-deficient sample, the concentration of oxygen vacancies appears to be increased at the grain boundaries.
- The Auger parameter shows upon reduction an evolution of the Y-O bond towards a more covalent one, this evolution being modulated with the presence of ZrO_2.

I - INTRODUCTION

Point defects play an important rôle in the macroscopic properties of ceramics. These point defects can either be structural defects (vacancies, interstitials, lattice distortions), or they can be due to the chemical substitution of foreign cations with different ionic radius and coordination. However, the relationship between the structure of the defects and the resulting properties is not well understood, although it constitutes a promising way to set up high performance ceramics. Moreover, the structure of non-stoichiometric oxides is still not very well known / 1 /. Much work is needed to get a better insight into the electronic and atomic changes induced by the production of oxygen vacancies in oxides.

Yttrium oxide is a ceramic with high melting point, high resistivity, which crystallizes into the C-type rare earth sesquioxide structure. Only a few studies deal with the defect structure of this oxide,

which is widely used as a dopant in ZrO_2 for stabilization. Most of these studies are devoted to electrical conductivity measurements / 2, 3, 4, 5 /. In a previous paper / 6 /, we have shown that pure yttria exhibits a quite different fracture behavior when it is non-stoichiometric (oxygen deficient) compared to the stoichiometric case.

On the stoichiometric sample, a transgranular fracture path occurs, whereas in the oxygen deficient ones, the fracture features are intergranular.

This paper deals with the structure of oxygen-rich or deficient yttria ceramics produced by redox processes at high temperatures / 7 /. These ceramics are either pure or doped with zirconia. Indeed yttria is able to dissolve tetravalent cations such as Zr, without change in the crystallographic structure / 8/.

The local geometric structure around an yttrium atom located in the bulk was probed using EXAFS (Extended X-ray absorption fine structure) above the K-absorption edge of yttrium. The results are extensively reported in another paper / 9 / ; we only summarize them here.

The local electronic structure around yttrium and oxygen, at the surface, was investigated using X-ray photoemission to get insight into the nature of the Y-O bond and its modification with oxygen content.

Both methods give an averaged information on a large area (a few mm^2) of the sample, and do not allow determination of the structure (both geometric and electronic) at the grain boundaries, compared to the bulk of the grains. Therefore scanning electron microscopy was used to get informations on processes occuring at the grain boundaries.

The results show that large concentrations of oxygen vacancies may be produced in reduction condition, for pure yttria as well as ZrO_2-doped yttria.

When oxygen vacancies are introduced, there is no apparent change in the Y-O and Y-Y bond lengths, but there is a charge transfer from the anions to the cations, leading to a more covalent Y-O bond. For pure yttria, scanning electron microscopy shows that the surface potential at the grain boundaries is different from that of the bulk, indicating that oxygen vacancies are preferentially segregated at the grain boundaries.

II - MATERIALS AND METHOD

II.1 - Samples

Pure Y_2O_3 (5N) * and 14 wt % (23 mol %) ZrO_2-doped yttria powders were sintered under high isostatic pressure (HIP) : 1450°C, 150 MPa for 45 mn. Zr-doped powders were synthetized using a precipitation method. The ZrO_2 powder ** was dispersed into an aqueous solution of yttrium nitrate. Precipitation of yttrium hydroxide was then obtained by reaction with ammonium hydroxide, followed by calcination.

---

* Rhône-Poulenc, France

** Criceram, France

The green body was then cut into pellets of thickness 1 mm. The samples used for scanning electron microscopy were mechanically polished. All samples were first annealed for 2 hours at 1500°C (oxidation heat treatment) in the room atmosphere, in order to bleach the intrinsic oxygen vacancies and the residual stresses resulting from the sintering process and to produce oxygen rich samples (white color).

Some of them were heated at 1200°C in vacuum (10^{-6} torr) to obtain stoichiometric samples, according to the conductivity σ versus Log P_{O_2} plots measured by Tallan et West / 2 /.

Others were heated at 1700°C in vacuum (10^{-6} torr). This latter treatment corresponds to a dissociation condition of the oxide / 2, 10 / leading to its reduction. Therefore a rather large number of oxygen vacancies is expected, at least in the case of the pure Y_2O_3. This latter treatment (reduction heat treatment) led to black samples.

The Zr concentration was chosen according to the phase diagram of the yttria-zirconia system / 11 /. 14 wt % ZrO_2 is located at the boundary of the one solid solution (substituted Zr in Y_2O_3) field, and a two solid solution (Zr in Y_2O_3 and Y in ZrO_2) field. Therefore, only the doped sample annealed at 1700°C is constituted by a single phase, as verified by X-ray diffraction. The lattice parameter (10.56 Å) is found to be smaller than in the case of the pure Y_2O_3 (10.604 Å), as reported by Scott / 8 /.

II.2 - Methods : photoelectron spectroscopy

X-ray photoelectron spectroscopy is a very sensitive tool for measuring chemical shifts of electron binding energy, produced by modifications of the electronic environment. However, this technique is difficult to apply to the case of Y-O bonds in samples with different oxygen stoichiometry : this arises from the small chemical shifts of the Y3d peak in the photoelectron spectrum, and from a propensity for charge building up under the exciting beam.

To overcome such problems the Auger parameter introduced by Wagner / 12, 13 /, can be used. This parameter is defined as the difference between the kinetic energy of the Auger electron (ijk) and that of the photoelectron emitted from the inner shell i, as measured on the photoelectron spectrum :

$$A = E_{kin}\,(ijk) - E_{kin}\,(i)$$

It depends on the incident photon energy $h\nu$. For this reason the modified Auger parameter A' was introduced :

$$A' = E_{kin}\,(ijk) + E_B(i) = A + h\nu$$

where $E_B(i)$ is the binding energy of the photoelectron emitted from the shell i. Using Koopman's approximation, it can be shown that the Auger parameter variation ΔA for two different chemical environments is twice the variation of the extraatomic relaxation energy arising from the decrease of the screening charge for the electrons involved in the chemical bond when a positive hole is left on the inner shell i. Hence

ΔA is directly related to the electronic polarization energy variation ΔE_{pol} resulting from the ionization of the inner shell i / 14-17 / :

$$\Delta A = 2\ \Delta E^{ea}_{relax}(i) = -\ 2\ \Delta E_{pol}$$

Data obtained on several silicates / 18 / showed a direct correlation between this polarisation energy and the polarizability α_o of the oxygen ion in the chemical environment considered :

$$\Delta A = -\ K\alpha_o$$

where K is a constant.

II.2 - Experimental set-up

Photoemission experiments were carried out in a VG Escalab Mark II with a base pressure around 5.10^{-11} mbar. In the analysis chamber a monochromatized X-ray source equipped with an aluminum anode was available ($h\nu$ =1486.6 eV). On the other hand, a conventional twin anode source could be used (AlKα and ZrLα). In all cases, the electrons emitted from the sample were energy filtered in a hemispherical analyser operated in the constant analyser energy mode, with a pass energy of 50 eV. In order to overcome sample charging under the incident photon beam, an electron flood gun (5 eV, 200 μA) was used. The working conditions of this gun were chosen so as to get for the O 1s photoelectron line recorded on the stoichiometric sample the same value as that of the same line on Al_2O_3 . Detection was made by a counting method ; data could be stored and processed using a DAD system.

Scanning electron microscopy was performed using a high resolution scanning reflection electron microscope (JSM 880-JEOL). This microscope is equipped with an immersion lens which allows one to reach 1.5 nm resolution in the secondary electron imaging (SEI) mode or 5 nm in the backscattered electron imaging (BEI) mode. Primary currents as low as 10^{-12} A could be used , as well as low accelerating voltage such as 1.7 kV.

III - RESULTS

III.1 - Photoemission results

The modified Auger parameters of respectively oxygen (A'_O) and yttrium (A'_Y) were measured for pure Y_2O_3 samples submitted to either the oxidation (1500°C air) or the reduction (1700°C vacuum) heat treatments, and for the ZrO_2-doped samples (14 wt %) submitted to the reduction heat treatment (1700°C vacuum).

A'_O is associated to the O 1s photoelectron line, and the O KLL Auger peak. A'_Y is associated to the Y3d photoelectron line, and the Y $L_3M_5M_5$ Auger peak. The latter line was obtained using the Bremsstrahlung X-ray background produced by the non monochromatized source. Indeed M levels can be considered as core levels in yttria, and therefore a good assumption is that the chemical shifts of the 3d levels and the 2p levels differ by only tenths of eV.

Figure 1 shows the photoelectron spectrum including the part extracted by the Bremsstrahlung background obtained on the pure oxidized Y_2O_3 sample.

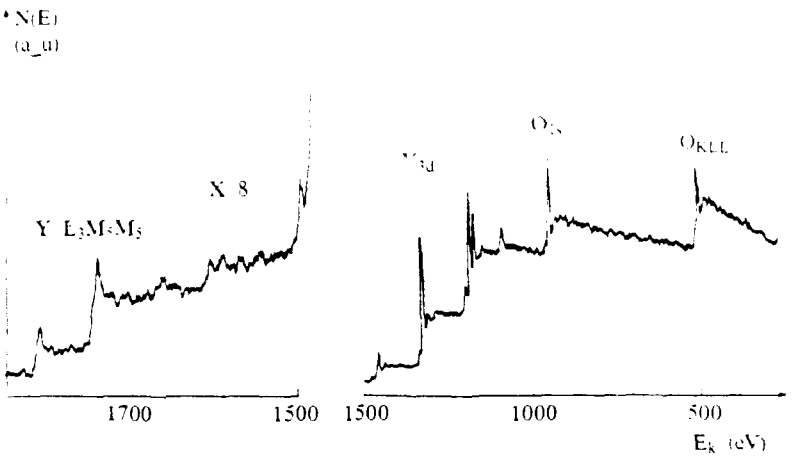

Figure 1. X-ray photoelectron spectrum of Y_2O_3 showing the $L_3M_5M_5$ Y-Auger peak and the Y-3d photoelectron line, used to calculate the Auger parameter (AlKα radiation).

For a given sample, A'_O and A'_Y do not vary with the experimental conditions : AlKα or ZrLα exciting line, charge compensation or not with the flood gun, within an uncertainty of 0.4 eV. In all cases, the pure reduced Y_2O_3 has the largest modified Auger parameters (A'_O = 1041.5 eV, A'_Y = 1895 eV), the pure oxidized Y_2O_3 the smallest (A'_O = 1037 eV, A'_Y = 1893.3 eV). The doped reduced Y_2O_3 has Auger parameters located inbetween, but closer to that of the pure reduced Y_2O_3 (A'_O = 1040 eV, A'_Y = 1894.6 eV).

The difference of the modified Auger parameters when going from the pure reduced Y_2O_3 to the pure oxidized Y_2O_3 are :

$$\Delta A'_O \simeq 4.5 \text{ eV} \quad \text{and} \quad \Delta A'_Y \simeq 1.7 \text{ eV}$$

On the other hand, considering the reduced samples, the difference of the modified Auger parameter when going from pure Y_2O_3 to doped Y_2O_3 are :

$$\Delta A'_O \simeq -1,2 \text{ eV} \quad \text{and} \quad \Delta A'_Y \simeq -0.4 \text{ eV}$$

III.2 - Scanning electron microscopy

The backscattered electron image (BEI) and the secondary electron image (SEI) of respectively the pure reduced Y_2O_3 and the doped reduced Y_2O_3 (14 wt % ZrO_2) are shown on fig. 2 (a,b) and fig. 3 (a,b).

For both samples, the BEI image reveals the grain structure at the surface (fig. 2.a and fig. 3.a). The contrast arises from crystalline effects / 19 /. Note that the grain size is slightly smaller (x 1/3) in the case of the doped reduced sample.

On the doped reduced Y_2O_3, the SEI image is similar to the BEI one, only the relative contrasts between the grains are different (fig. 3.b).

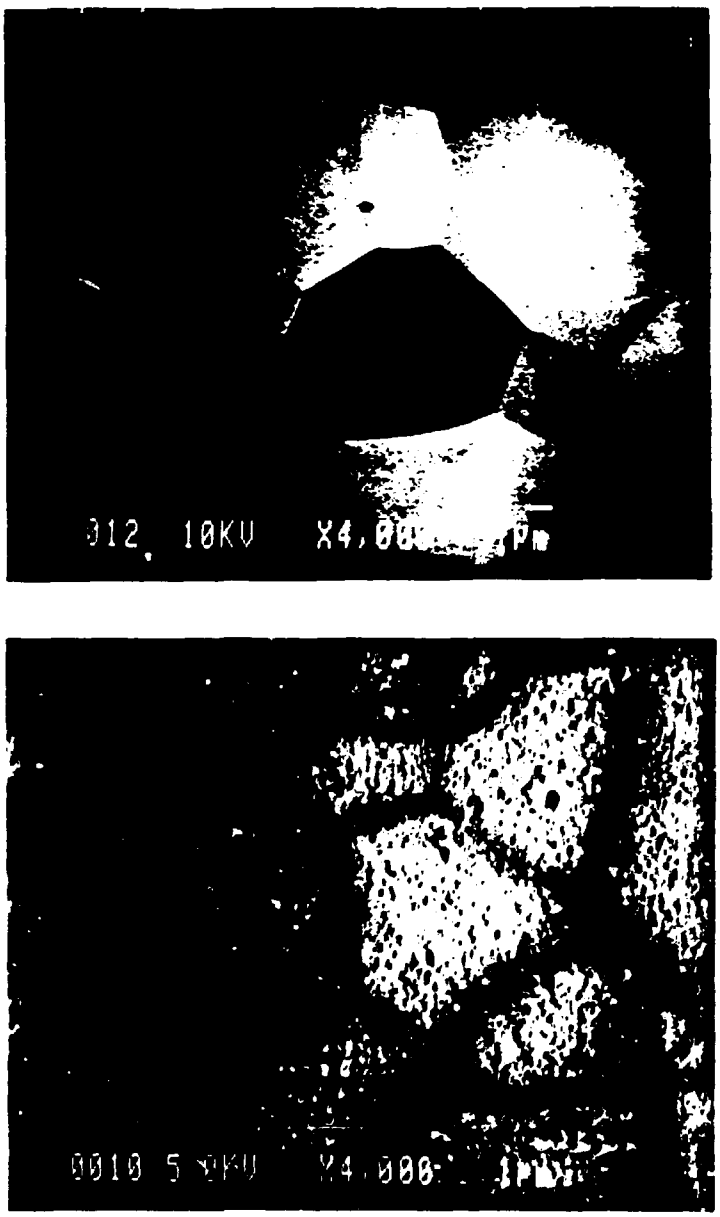

Figure 2. Scanning electron images of pure reduced Y_2O_3.
(a) BEI mode ; (b) SEI mode.

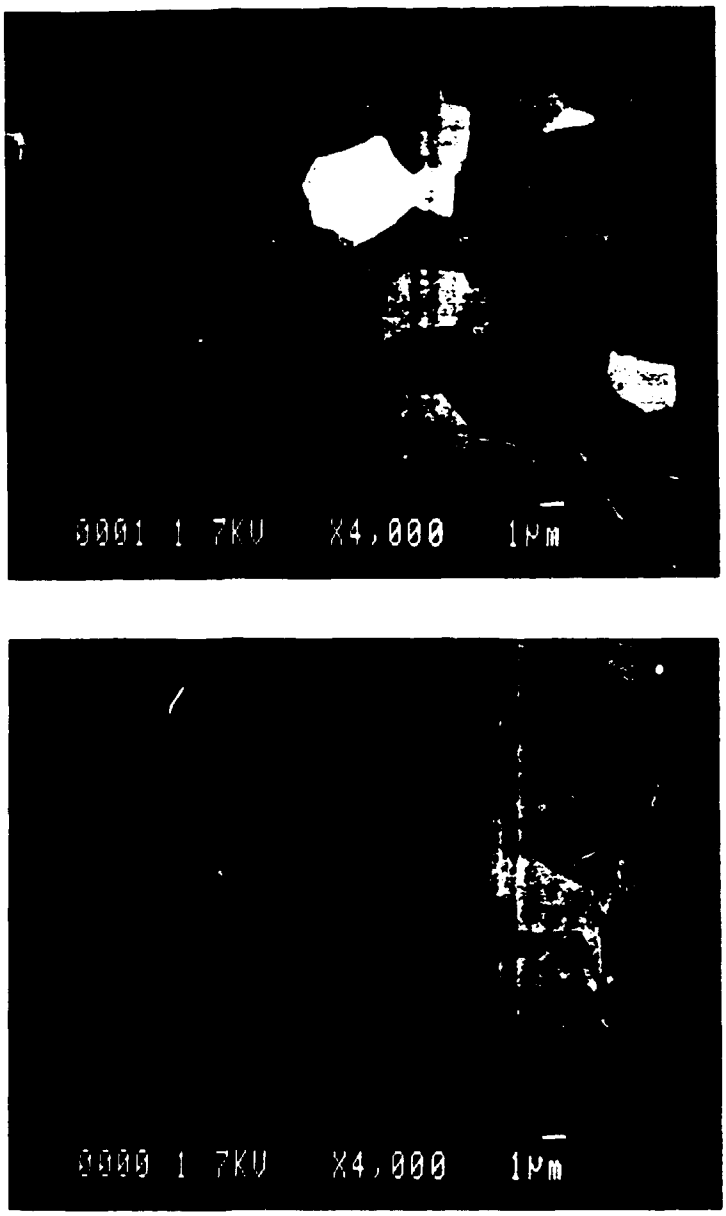

Figure 3. Scanning electron images of doped reduced Y_2O_3.
(a) BEI mode ; (b) SEI mode.

In the case of the pure reduced Y_2O_3, the SEI image is quite different : all grains have the same contrast, and along the grain boundaries a dark line can be observed (fig. 2.b).

These images were obtained without coating the samples. The experimental conditions : accelerating voltage and primary current ($I = 5.10^{-11}$ A) were chosen to avoid sample charging. Using the same conditions, it was possible to get a BEI image on the pure oxidized sample, but charging effects dit not allow us to obtain a SEI image.

IV - DISCUSSION

Yttrium oxide crystallizes into the C-type cubic rare earth sesquioxide structure. This structure is closely related to the fluorite structure. In the fluorite lattice, each cation is surrounded by a cube of eight anions. The C-type structure can be derived by removing one-quarter of the anions and slightly rearranging the remaining ions. For 25 % of the cations, the vacancies lie along a body diagonal and the anions are located at the vertices of a slightly distorted octahedron. For the remaining cations, the vacancies lie along a face diagonal resulting in distorted octahedra. In such a structure, yttrium is six-fold coordinated.

The yttrium oxide structure, in the stoichiometric composition, contains ordered empty anionic sites. Therefore excess oxygen atoms are expected to be incorporated into the lattice either by oxidation heat treatment, or by introducing foreign cations with a higher valency than yttrium. Y_2O_3 can dissolve different amounts of oxides with tetravalent cations such as ZrO_2 (20 mol % ZrO_2 at 1500°C). The solubility limit increases with temperature (24 mol % ZrO_2 at 2000°C) / 20 /. Addition of tetravalent Zr^{4+} cations induces interstitial anions, whose mobility is high / 21 /.

IV.1 - Bulk defect structure of pure and doped yttria

Most experimental studies on yttrium oxide defect structure are based on conductivity measurements / 2, 3, 4, 5, 22 /. They give a description of the defect structure in terms of isolated point defects without interaction, at the thermodynamic equilibrium. In fluorite-like oxides, the cation sublattice is considered very stable, and the cations are much less mobile than the anions. Therefore the predominant defects in Y_2O_3 are located on the oxygen sublattice. In pure yttria, the most probable point defects are anion Frenkel pairs O_i'', $V_o^{\cdot\cdot}$ / 22 /. It has been shown / 3, 4, 5 / that the conductivity strongly depends on water pressure, pointing out the role of $H^{\cdot}$ which compensates the positive O_i'' defects if the water pressure is important.

For ZrO_2-doped Y_2O_3, oxygen interstitials have been observed / 21, 23 / as expected from the C-type cubic crystallographic structure.

The detailed structure of defects in anion deficient fluorite oxides is not known, but the usual defect arrangement is based on the pairing of empty anion sites accross the diagonal of the cubic cation coordination polyhedron / 1 /.

The local geometric structure around an yttrium atom located in the bulk was probed using EXAFS (Extended X-ray Absorption Fine Structure) above the K absorption edge of yttrium, in the pure and doped reduced yttria samples of this work / 9 /.

Main results are the following :

<u>Pure Y_2O_3</u> : In reduction conditions, an appreciable number of oxygen vacancies can be introduced ($\sim$ 10 % in the first coordination shell around an yttrium atom). The production of such defects does not lead to any apparent reorganization of the lattice in the conditions

explored : the bond lengths remain constant within the accuracy of the method (2.10^{-2} Å) but static disorder in the first coordination shell increases in anion deficient samples.
Doped Y_2O_3 : For the same reduction treatment, the number of oxygen vacancies in the first coordination shell ($\sim$ 30 %) is larger, and the static disorder much weaker than for pure Y_2O_3, while the bond lengths remain constant too. Then, there is a competing process between the introduction of oxygen-excess by doping with a tetravalent cation, and the production of anion vacancies upon reduction. In doped fluorite oxides, the oxygen diffusion coefficients are enhanced / 1, 20 /. This could account for the higher deficit of oxygen in Zr-doped yttria, compared to the case of pure yttria with the same reduction heat treatment.

IV.2 - Electronic structure of pure and doped yttria surfaces

In a scheme of isolated point defects, as anionic vacancies $V_O^{\cdot\cdot}$ (or $V_O^{\cdot}$) as well as dopant ions $Zr_Y^{\cdot}$ (in substitution) bear positive effective charges, the perturbation of charge equilibrium in the bulk must be restored by the introduction of negative species, such as delocalized electrons in the conduction band.

In other terms, an electron transfer must occur for charge compensation. This is shown by the XPS results, which concern the surface of the ceramic (20-30 Å). For the purpose of this part, we will assume that the conclusions on the local geometric structure obtained by EXAFS, which concern the bulk of the ceramic, are qualitatively valid at the surface. SEXAFS (surface EXAFS) measurements are currently in progress to make this point precise. However, oxygen vacancies exist at the surface, but may be in a different concentration to that in the bulk. The main difference between bulk and surface is that the surface need not necessarily be neutral, and the local electronic structure around either an yttrium or an oxygen atom may be quite different in the bulk or at the surface / 24 /.

As mentioned in II.2, in an ionic bond model, which can be applied to be case of an ionocovalent oxide such as Y_2O_3, the variation of Auger parameter can be related to the electronic polarization energy variation and to the polarizability variation of the oxygen ion.

In the case of the reduced samples (pure or doped) the oxygen Auger parameter is larger than for the oxidized pure sample. This result shows that the creation of oxygen vacancies leads to a charge redistribution which makes the Y-O bond more covalent on average, and which corresponds to a decrease in the mean oxygen polarizability. A charge transfer occurs from the anion to the cation. The same conclusion can be obtained considering the yttrium Auger parameter, whose variation is weaker.

This conclusion concerning the decrease of the ionic character of the oxide when reducing was confirmed by the study of the oxygen KLL Auger lineshape, and by the energy of the final state of the ion in the O KLL Auger transition / 9, 25 /.

As far as the reduced doped Y_2O_3 sample is concerned, the Auger parameters of Y and O indicate a charge transfer at most as great as that observed in the pure sample having experienced the same reduction treatment, although the oxygen deficit around Y is larger. That would imply that the change of ionicity of the Y-O bond is also related to the static disorder in the first coordination shell.

IV.3 - Microscopic aspects of the surface modifications induced by a reduction heat treatment

The EXAFS investigations and the XPS experiments show differences in the local geometric structure around an yttrium atom, as well as in the local electronic structure around both oxygen and yttrium. This information is averaged over the part of the surface irradiated by the X-ray beams (i.e., for EXAFS : 2 cm x 5 mm and for XPS : 8 mm x 2 mm).

As these ceramics are polycrystalline it is necessary to investigate the spatial homogeneity of this information. These microscopic observations have been obtained by scanning electron microscopy.

The behavior of uncoated yttrium oxide under an electron beam is quite different when the sample is stoichiometric or oxygen deficient. This different behavior toward charging up under the beam has been observed for pure Y_2O_3 in a previous paper / 6 /.

On the doped reduced sample, the differences in the contrasts of the different grains observed on the backscattered electron image and in the secondary electron image arise from channeling of the primary electron beam / 26 /. This effect modulates the backscattering coefficient of the primary beam, and can be observed also in the secondary electron imaging mode (SEI), due to the contribution of backscattered electrons to the total intensity of the detected electrons.

The pure reduced sample exhibits a quite different type of contrast when observed in SEI. The crystalline contrast is no longer observed, but a black zone appears along the grain boundaries. This contrast, similar to a voltage contrast, can be attributed to a modification of the surface potential in the neighborghood of the grain boundaries. The grain boundaries are transition regions between crystals with the same nature but with different crystallographic orientation. Therefore defects may find favored sites to diffuse. Thus, in the case of the pure oxygen deficient sample, oxygen vacancies could diffuse and give rise because of their effective charge to a local potential, which could be at the origin of the contrast observed in the secondary electron image. This contrast was observed to disappear under oxidation conditions / 6 /, indicating that it is related to the presence of oxygen vacancies which are segregated at the grain boundaries of the pure reduced Y_2O_3 sample.

However, this electrical activity at the grain boundaries is not observed on the doped reduced sample, which is known to contain more anionic vacancies than the pure reduced one, as deduced from the EXAFS results.

This would imply that, in the case of the doped reduced samples the anionic vacancies are not so strongly segregated at the grain boundaries. This may be due to a competitive segregation of Zr at the grain boundaries. The difference in the grain growth in the doped sample supports this hypothesis. Indeed for the same H.I.P. processing and the same subsequent heat treatment, the mean grain size in the doped reduced sample is three times smaller on average than in the pure reduced one, indicating that Zr plays an important role in the grain boundary motion.

Furthermore, this result concerning the segregation of vacancies in the pure and doped Y_2O_3 has to be related to the differences observed in the local geometric structure around an yttrium atom in the pure and doped yttria. In the doped reduced sample, the number of oxygen vacancies is larger, and the static disorder much less important than in the pure reduced one, but no point defect association or ordering can be deduced from the EXAFS results, as outlined by Tang et al. / 27 /.

However it is known that, when the concentration of defects is high, the induced disorder may be stabilized either by defect clustering or aggregation, or by the elimination of point defects with the formation of extended planar defects. Defect clustering has been observed for example in oxygen deficient CeO_2 (doped with Y^{3+}), which crystallizes in the fluorite structure.

Elimination of point defects with formation of extended planar defects, such as shear planes, has been observed in oxygen deficient titanium oxide /1/.

The formation of such extended defects in the doped reduced Y_2O_3 ceramics could on the one hand explain the lack of static disorder in the first coordination shell around Y, compared to the case of the pure reduced samples, and on the other hand the difference in the defect segregation at the grain boundaries, which changes their electrical activity, and therefore their SEI contrast. Further experiments on grain boundaries must shed light on these hypothesis.

V - CONCLUSION

Surfaces of oxygen deficient yttrium oxide, pure or doped (14 wt % ZrO_2), were studied by means of X-ray photoelectron spectroscopy and scanning electron microscopy.

After a reduction heat treatment (1700°C under vacuum) an important concentration of oxygen vacancies is produced as shown for the bulk by the EXAFS measurements, the oxygen deficiency depending on the doping.

The presence of these oxygen vacancies leads to a modification of the local electronic distribution of the surface around both Y and O. A partial charge transfer from the anion to the cation occurs, leading to a more covalent Y-O bond.

However this information is averaged over several grains of the polycrystalline ceramics. Using scanning electron microscopy, an inhomogeneity in the anionic vacancies concentration was observed, depending on the presence of altervalent substituting cations (Zr).

An electrical activity of the grain boundaries is detected in the case of pure reduced Y_2O_3 : oxygen vacancies are strongly segregated at the grain boundaries. However, this electrical activity cannot be seen for doped reduced Y_2O_3 in which the anionic vacancies concentration is larger.

This result has to be related to some defect rearrangement in doped reduced Y_2O_3, like defect clustering or formation of extended defects (shear planes), in agreement with the differences in the static disorder obtained by the EXAFS experiments.

REFERENCES

/1/ C.R.A. Catlow, 'Defect clustering in nonstoichiometric oxides', in 'Non stoichiometric oxides', 61-98. ed. by O. Toft Sorensen. Academic Press, New York (1981).

/2/ N.M. Tallan, R.W. Vest, 'Electrical properties and defect structure of Y_2O_3', J. Am. Ceram. Soc., 49 (8), 401-404 (1966).

/3/ T. Norby, P. Kofstad,'Direct Current Conductivity of Y_2O_3 as a function of water vapor pressure', J. Am. Ceram. Soc., 69 (11) 780-783 (1986).

/4/ T. Norby, P. Kofstad, 'Electrical conductivity of Y_2O_3 as a function of oxygen partial pressure in wet and dry atmospheres', J. Am. Ceram. Soc., 69 (11), 784-789 (1986).

/5/ T. Norby, P. Kofstad, 'Proton and native-ion conductivities in Y_2O_3 at high temperatures', Sol. Stat. Ionics, 20, 169-184 (1986).

/6/ F. Jollet, Ph. Maire, M. Gautier, J.P. Duraud, C. Le Gressus, 'Influence of stoichiometry on the electrical and mechanical behavior of yttrium oxide ceramics', J. Am. Ceram. Soc., 71, (9), C396-C398 (1988).

/7/ H.L. Tuller, 'Thermodynamics and defect structure of non stoichiometric oxides', in 'Non-Stoichiometric oxides', 2-59, ed. by O. Toft Sorensen, Academic Press, New York (1981).

/8/ M.G.SCOTT, 'Phase relationships in the zirconia-yttria system', J. of Materials Science, 10, 1527-1535 (1975).

/9/ J.P. Duraud, F. Jollet, N. Thromat, M. Gautier, Ph. Maire, C. Le Gressus, E. Dartyge, 'Non-stoichiometry of pure and Zr-doped yttria ceramics : an EXAFS and XPS study', submitted to J. Am. Ceram. Soc.

/10/ R.C. Anderson, in 'High temperature oxides', ed. by M. Aper, Academic Press, New York, 1-40 (1970).

/11/ P. Duwez, F.H. Brown, F. Odell, 'The zirconia-yttria system', J. Electrochem. Soc., 98, 350-352 (1951).

/12/ C.D. Wagner, 'Auger parameter in electron spectroscopy for the identification of chemical species', Anal. Chem., 47, 1201-1203 (1975).

/13/ C.D. Wagner, D.E. Passoja, H.F. Hillery, T.G. Kinisky, H.A. Six, W.T. Jansen, J.A. Taylor, 'Auger and photoelectron line energy relationships in aluminium-oxygen and silicon-oxygen compounds', J. Vac. Sci. Technol., 21 (4), 933-944 (1982).

/14/ S. Kohiki, S. Ozaki, T. Hamada, 'Characterization of silicon compounds using the Auger parameter in X-ray photoelectron spectroscopy (XPS)', Appl. Surf. Science, 28, 103-110 (1987).

/15/ N.F. Mott, R.W. Geviney, 'Electronic Processes in Ionic Crystals', Clarendon, Oxford, 1948.

/16/ C.D. Wagner, 'Chemical shifts of Auger lines, and the Auger parameter', Faraday Disc. Chem. Soc., 60, 291-301 (1975).

/17/ C.D. Wagner, A. Joshi, 'The Auger parameter, its utility and advantages : a review', J. of Electron Spectroscopy and Related Phenomena, 47, 283-313 (1988).

/18/ R.H. West, J.E. Castle, 'The correlation of the Auger parameter with refractive index : an XPS study of silicate using ZrLα radiation', Surf. Interf. Analysis, 4 (2), 68-75 (1982).

/19/ H. Niedrig, 'Electron backscattering from thin films', J. Appl. Phys., 53 (4), R15-R49 (1982).

/20/ T.H. Etsell, S.N. Flengas, 'The electrical properties of solid oxide electrolytes', Chem. Rev., 70, 339-376 (1970).

/21/ K. Ando, Y. Oishi, 'Oxygen self diffusion in Y_2O_3 and Y_2O_3-ZrO_2 solid solutions', NATO-ASI, ser. B, 129, 203-215 (1985).

/22/ Ph. Odier, J.P. Loup, 'An unsual technique for the study of non-stoichiometry : the thermal emission of electrons. Results for Y_2O_3 and TiO_2', J. of Solid State Chem., 34, 107-119 (1980).

/23/ R. Bratton, 'Defect structure of Y_2O_3-ZrO_2 solid solutions', J. Am. Ceram. Soc., 52, 213 (1969).

/24/ A.M. Stoneham, 'Ceramic Surfaces : theoretical studies', J. Am. Ceram. Soc., 64 (1), 54-60 (1981).

/25/ C.D. Wagner, D.A. Zatko, R.H. Raymond, 'Use of the oxygen KLL Auger lines in identification of surface chemical states by electron spectroscopy for chemical analysis', Anal. Chem., 52, 1445-1451 (1980).

/26/ D.C. Joy, D.E. Newbury, D.L. Davidson, 'Electron channeling patterns on the scanning electron microscope', J. Appl. Phys., 53 (8), R81-R122 (1982).

/27/ C. Tang, P. Georgopoulos, J.B. Cohen, 'Study of extended X-ray absorption fine structure for possible use in examining local atomic arrangements in oxides', J. Am. Ceram. Soc., 65 (12), 625-629 (1982).